Progress In Electromagnetics Research B, Vol. 3, 35–46, 2008

BREAST CANCER DETECTION USING A HYBRID FINITE DIFFERENCE FREQUENCY DOMAIN AND PARTICLE SWARM OPTIMIZATION TECHNIQUES

S. H. Zainud-Deen, W. M. Hassen, E. M. Ali, K. H. Awadalla and H. A. Sharshar

Faculty of Electronic Engineering
Menoufia University
Menouf, Egypt

Abstract—A hybrid technique based on Finite-difference frequency domain and particle swarm optimization techniques is proposed to reconstruct the breast cancer cell dimension and determines its position. Finite-difference frequency domain is formulated to calculate the scattered field after illuminating the breast by a microwave transmitter. Two-dimensional and three-dimensional models for the breast are used. The models include randomly distributed fatty breast tissue, glandular tissue, 2-mm thick skin, as well as chest wall tissue. The models are characterized by the dielectric properties of the normal breast tissue and malignant tissue at 800 MHz. Computer simulations have been performed by means of a numerical program; results show the capabilities of the proposed approach.

1. INTRODUCTION

Breast cancer is the most frequently diagnosed cancer in women. It is the second leading cause of cancer death in women after lung cancer. Detection of early stage tumor reduces the breast cancer mortality rate. Screening programs have been introduced across Egypt to encourage women to have regular mammograms. X-ray mammography is currently the most effective screening modality for detecting clinically occult breast cancers. Mammography fulfills almost all requirements to be an efficient imaging tool [1]. However, X-ray mammography has the following shortcomings [2, 3]:

1. It has difficulties in detecting breast tumors at their earlier stages.

2. It has decreased effectiveness in cases of women with dense breasts and also in detecting tumors located near the chest wall or underarm.
3. Using ionizing X-rays may destroy the tissue they penetrate.
4. The discomfort of the patients because of breast compression, and the relatively expensive cost.

Complementary non-ionizing imaging methods exist today. The most important ones are ultrasound and magnetic resonance imaging (MRI) with contrast enhancement, but no one of these methods is used in routine cancer screening. These methods cannot detect the early signs of cancer, so they have importance in later diagnostics to verify the malignity of the breast tissue [4–7].

Microwave imaging can be used effectively for the detection of biological anomalies like tumor at an early curable stage. It can be one of the needed imaging modalities in the future. This is because microwave imagining has a strong potential to detect tumor due to the high dielectric contrast between malignant and glandular breast tissues in the microwave range [6]. Also, microwave imaging is a non-ionizing method which probably will be rather inexpensive compared to MRI and safer compared to X-ray. Versions of video pulse radars were first introduced for medical applications as a means to detect malignancy in internal biological tissues by Hagness et al. [8–10]. Fear et al. [11–13] demonstrated the feasibility of detecting and localizing small tumors in three dimensions.

The detection of the cancer and its position represents a complex inverse scattering problem that needs to be solved iteratively. That means the error between the measured data and the scattered fields computed from the trial solution is minimized at the end of the iteration, and the trial solution is then progressively adjusted towards the size and the position of the cancer. It is well-known that traditional deterministic techniques [15, 16] used for fast reconstruction of microwave images suffer from a major drawback, where the final image is highly dependent on the initial trial solution. In addition, it is often difficult to decide the adequacy of the initial trial solution for ensuring the correctness of the final solution. To overcome this obstacle, population based stochastic methods such as the genetic algorithm (GA) and particle swarm optimizer (PSO) have become attractive alternatives to reconstruct microwave images [17–19]. These techniques consider the imaging problem as a global optimization problem by imparting each individual within the population with its own fitness value as per the objective function defined for the problem, and reconstruct the correct image by searching for the optimal solution through the use of either rivalry or cooperation strategies in the

problem space. In this paper, a hybrid solution based on the finite-difference frequency-domain (FDFD) and the particle swarm optimizer (PSO) techniques are used to detect and determine the position of the cancer.

This paper is organized as follows. In Section 2, the methods that are used in the simulation are shown, where the 2-D and the 3-D breast modals simulated using (FDFD) to calculate the scattered field and using (PSO) to reconstruct the cancer cell position. Section 3, shows the models that are used for the breast and the tumor. In Section 4, numerical results are shown to demonstrate the efficiency of the technique. Conclusions are presented in Section 5.

2. PROBLEM FORMULATION

Recently, the finite-difference frequency-domain method has received considerable interest as an efficient, full-wave numerical solution for electromagnetic problems. The finite difference frequency domain is simple in formulation and most flexible in modeling arbitrarily shaped inhomogeneously filled and anisotropic scatterers [20–22].

Maxwell's curl equations in frequency domain can be written as:

$$\begin{aligned} \nabla \times \overline{\mathrm{E}}_{\mathrm{total}} &= -j\omega\mu\overline{\mathrm{H}}_{\mathrm{total}} \\ \nabla \times \overline{\mathrm{H}}_{\mathrm{total}} &= (j\omega\varepsilon + \sigma)\,\overline{\mathrm{E}}_{\mathrm{total}} \end{aligned} \tag{1}$$

Defining the total fields as the sum of the incident and the scattered fields:

$$\overline{\mathrm{E}}_{\mathrm{total}} = \overline{\mathrm{E}}_{\mathrm{inc}} + \overline{\mathrm{E}}_{\mathrm{scat}}, \quad \text{and} \quad \overline{\mathrm{H}}_{\mathrm{total}} = \overline{\mathrm{H}}_{\mathrm{inc}} + \overline{\mathrm{H}}_{\mathrm{scat}} \tag{2}$$

where $\overline{\mathrm{E}}_{\mathrm{inc}}$, and $\overline{\mathrm{E}}_{\mathrm{scat}}$ are the incident and the scattered field, respectively. The incident field is the field which propagates in computation domain when no scatterers exist. If the background of the computation domain is free space, then the incident fields are defined by the equations:

$$\nabla \times \overline{\mathrm{E}}_{\mathrm{inc}} = -j\omega\mu_o\overline{\mathrm{H}}_{\mathrm{inc}}, \quad \text{and} \quad \nabla \times \overline{\mathrm{H}}_{\mathrm{inc}} = j\omega\varepsilon_o\overline{\mathrm{E}}_{\mathrm{inc}} \tag{3}$$

Then Maxwell's curl equations can be rewritten as:

$$\nabla \times \overline{\mathrm{E}}_{\mathrm{inc}} + \nabla \times \overline{\mathrm{E}}_{\mathrm{scat}} = -j\omega\mu\overline{\mathrm{H}}_{\mathrm{inc}} - j\omega\mu\overline{\mathrm{H}}_{\mathrm{scat}} \tag{4}$$

$$\nabla \times \overline{\mathrm{H}}_{\mathrm{inc}} + \nabla \times \overline{\mathrm{H}}_{\mathrm{scat}} = (j\omega\varepsilon + \sigma)\,\overline{\mathrm{E}}_{\mathrm{inc}} + (j\omega\varepsilon + \sigma)\,\overline{\mathrm{E}}_{\mathrm{scat}} \tag{5}$$

From Equations (3), (4), and (5)

$$\nabla \times \overline{\mathrm{E}}_{\mathrm{scat}} + j\omega\mu\overline{\mathrm{H}}_{\mathrm{scat}} = j\omega\,(\mu_o - \mu)\,\overline{\mathrm{H}}_{\mathrm{inc}} \tag{6}$$

$$\nabla \times \overline{\mathrm{H}}_{\mathrm{scat}} - (j\omega\varepsilon + \sigma)\,\overline{\mathrm{E}}_{\mathrm{scat}} = (j\omega\,(\varepsilon - \varepsilon_o) + \sigma)\,\overline{\mathrm{E}}_{\mathrm{inc}} \tag{7}$$

Decompose the vector equations to x, y, and z components and obtain six scalar equations. These equations are used to construct the 2D and 3D finite-difference frequency-domain method equations by replacing the partial derivatives with the center-difference approximation and introducing the subdivisions of space into cells of size Δx, Δy, and Δz. A finite volume of space consisting of N_x, N_y and N_z cells must contain both the scattering object and a sufficiently thick layer of free-space or "white space" separating the boundaries of the object on all sides from the boundaries of the cell space. The outer boundary of the cell space is designed to absorb any energy incident upon it, by imposing the PML layers [23]. More details about the FDFD can be found in [20–22]. A general MATLAB code based upon the above analysis were developed by the authors. All evaluations presented here are performed on a Pentium IV at 3.2 GHz with 2 GB of RAM.

The term Particle Swarm Optimization (PSO) refers to a relatively new family of algorithms that may be used to find optimal (or near optimal) solutions to numerical and qualitative problems. The PSO was introduced to the antenna engineering community by Robinson and Rahmat-Samii [24]. The basic principles in PSO are very simple. A set of moving particles (the swarm) is initially "thrown" inside the search space. Each particle has the following features: i) It has a position and a velocity. ii) It knows its position and the objective function value for this position. iii) It knows its neighbors, best previous position and objective function value. iv) It remembers its best pervious position. At each time step, the behavior of a given particle is a compromise between three possible choices: i) To follow its own way. ii) To go towards its best previous position. iii) To go towards the best neighbor's best previous position, or towards the best neighbor. The ith particle of the swarm can be represented by a D-dimensional vector, $X_i = (x_{i1}, x_{i2}, \ldots, x_{iD})^T$. The velocity (position change) of this particle, can be represented by another D-dimensional vector $V_i = (v_{i1}, v_{i2}, \ldots, v_{id})^T$. The best previously visited position of the ith particle is denoted as $P_i = (p_{i1}, p_{i2}, \ldots p_{iD})^T$. Defining "$g$" as the position of the best particle in the swarm (i.e., the g-th particle is the best), this compromise is formalized by the following equations:

$$v_{id}^{n+1} = v_{id}^n + cr_1^n \left(p_{id}^n - x_{id}^n\right) + cr_2^n \left(p_{gd}^n - x_{id}^n\right) \tag{8}$$

$$x_{id}^{n+1} = x_{id}^n + v_{id}^{n+1} \tag{9}$$

where $d = 1, 2, \ldots, D$; $i = 1, 2, \ldots, N$, and N is the size of the swarm; c is a positive constant, called acceleration constant; r_1, r_2 are random numbers, uniformly distributed in [0,1]; and $n = 1, 2, \ldots$ determine the iteration number. A detailed discussion of the particle swarm optimizer used in this paper is provided in [24].

By starting from a defined residual as the difference between the calculated scattered field, E_{scat} and the measured scattered field, E_{meas}, as

$$E_{diff} = E_{scat} - E_{meas} \tag{10}$$

The optimization will then be performed on the square norm F

$$F = ||E_{scat} - E_{meas}||^2 = \min, \tag{11}$$

The goal is then to find the global minimum of this function.

3. MODEL OF THE BREAST

The adult female human breast consists of two main tissue types. Adipose tissue stores fat in adiposities, large lipid-filled cells, and makes up the vast majority of the breast, while glandular structures allow for milk production and transport. The glandular tissue comprises a network of lobules and branching epithelial ducts, which connect the network that allows for milk delivery. In addition, systems of vascular, connective, and neural tissues reside among the glandular and fat structures. The connective tissues are often referred to as the breast stoma.

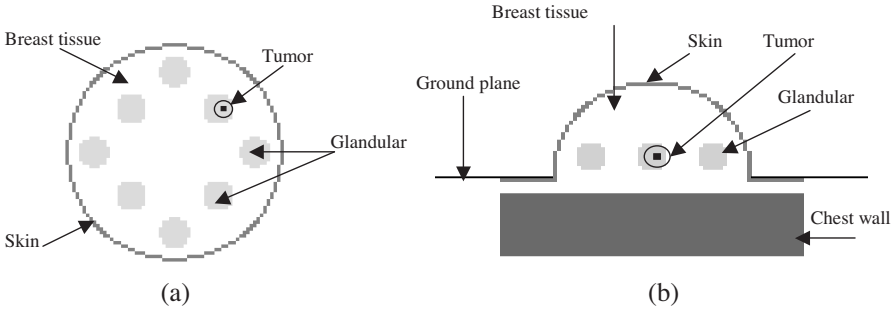

Figure 1. Two dimensional and three dimensional breast models, (a) the 2D model of the breast, (b) the 3D model of the breast.

In this paper, the 2D model of the breast is considered as an infinite inhomogeneous dielectric cylinder covered by a layer of skin. The cylinder axis is parallel to the z axis and its diameter is 100 mm. The model includes randomly distributed fatty breast tissue, glandular tissue, and 1.6 mm thick skin, as shown in Fig. 1(a). In the 3D model, the woman lies on her stomach with the breast naturally extending through a hole in the examination table (infinite size conducting

ground plane). The breast is a hemisphere with 75 mm in diameter. The model includes randomly distributed fatty breast tissue, glandular tissue, 5.3 mm thick skin, as well as chest wall, as shown in Fig. 1(b) and according to the anatomy of the breast given in [25, 26]. At 800 MHz, the relative permittivity "ε_r" and electrical conductivity "σ" for normal mammary tissues are around $\varepsilon_r \approx 16$ and $\sigma \approx 0.16$ s/m, respectively, while they are $\varepsilon_r \approx 57.2$ and $\sigma \approx 1.08$ s/m, respectively, for a malignant breast tumor [3, 27]. The contrast is 3.75 for the relative permittivity and 6.75 for the electrical conductivity. This high contrast gives rise to a large electromagnetic scattering signal when electromagnetic waves are applied to malignant tumor embedded in a normal tissue. The skin properties $\varepsilon_r \approx 36$ and $\sigma \approx 4$ s/m [2]. The chest wall properties in this paper is quite close to the properties of the tumor with the same percentage as in [28]. The mammary gland parameter is increased to 15% higher than the normal breast tissue [29]. The dielectric properties incorporated in the FDFD models are summarized in Table 1.

Table 1. Dielectric properties of breast tissues at frequency 800 MHz.

Tissue	Dielectric properties	
	Permittivity (ε_r)	Conductivity (σ)
Chest wall	57.2	2.1
Fatty breast tissue	16	0.16
Glandular tissue	18.4	0.184
Skin	36	4
Tumor	57.2	1.08

4. NUMERICAL RESULTS

In this section, numerical results of computer simulations that have been performed to assess the capabilities of the proposed approach have been reported and discussed. Due to the absence of the measured data, the FDFD technique is used to synthesize the measured scattered field values for the computation of forward solution. The scatterer is characterized by the dielectric properties of the normal breast tissue and malignant tissue at 800 MHz as given in Table 1. The domain is divided into equal sized sub cells. Inside this domain small malignant tissues have been embedded varied locations are represented by the dark shaded cells in all figures.

4.1. The 2D Results

The incident plane wave is assumed to be propagating in the direction normal to z-axis with the electric field vector polarized along the z axis which is taken to be parallel to the cylinder axis. The domain size that is used with the FDFD is 16×16 cm. The cell size is $\Delta x = \Delta y = 1.6$ mm, and the thickness of the PML layer is 10 cells. The swarm size that is used for the PSO is 30, and the number of iterations is 1000. Fig. 2 shows the construction of the breast after the hybrid method is used to detect and determine the positions of the tumors. A tumor ($\varepsilon_r = 57.2$, $\sigma = 1.08$ S/m) modeled as a square with side length of 1.6 mm was moved in different positions inside the breast model. Assuming the size of the tumor is fixed. The FDFD/PSO hybrid algorithm detected the position of the tumor in each case by searching only for the coordinates of the tumor. Then the size of the tumor is allowed to vary and the hybrid algorithm will have two goals to search for which are the coordinates of the tumor as well as the size of it. Fig. 3 shows different sizes of the tumor in different positions inside the breast which were explored by the FDFD/PSO algorithm.

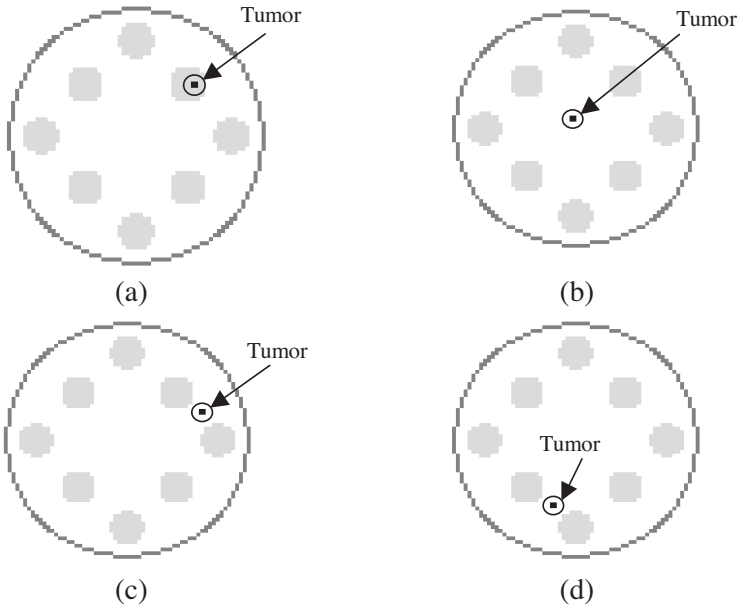

Figure 2. The location of the tumor for different cases in the 2D case.

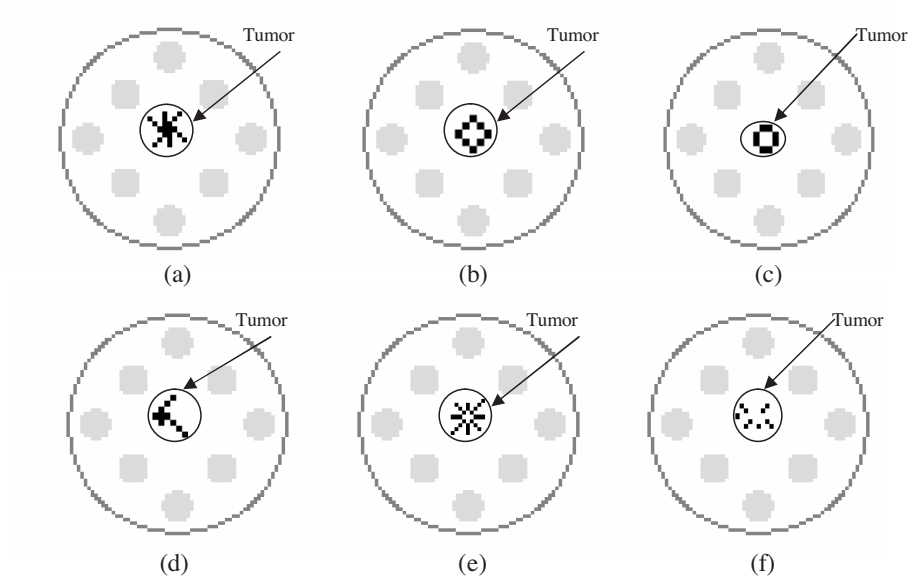

Figure 3. Different shapes of the tumor in different positions in the 2D case.

4.2. The 3D Results

The FDFD/PSO algorithm is used with the 3D breast model. The FDFD domain is $16 \times 16 \times 16$ cm, the cell size is $\Delta x = \Delta y = \Delta z = 5.3$ mm, the breast has a diameter 75 mm, and the skin is 5.3 mm thick and the thickness of the PML layer is 5 cells. In the 3D case the FDFD requires a huge sparse matrix to be inverted and this require longer time for iteration than the 2D case, so the goal of the PSO will be restricted here to find the coordinates of the tumor in the 3D breast model. The swarm size of the PSO is 20 and the number of iterations

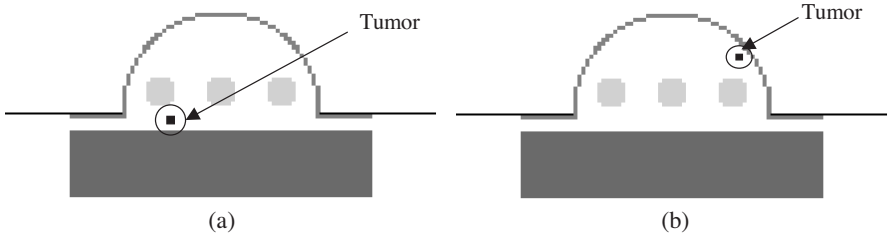

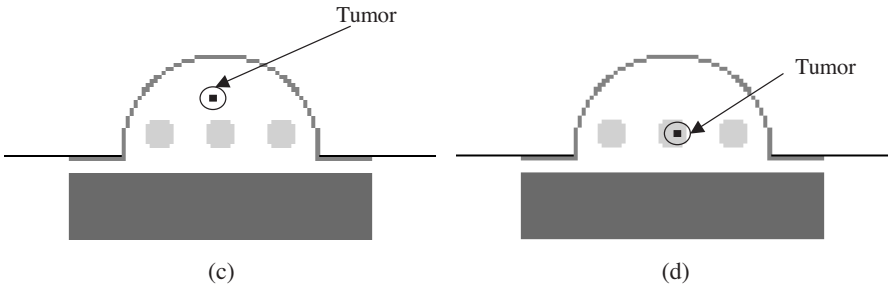

Figure 4. The location of the tumor in the 3D breast model, (a) the tumor very near to the chest wall, (b) the tumor near to the skin, (c) the tumor in the center of the breast, (d) the tumor inside the glandular.

that are used are 1000 Iterations. Fig. 4 shows the tumor positions in the breast model, near to the chest wall, near to the skin, in the center of the breast, and inside the glandular. In Figs. 2, 3 and 4, the malignant tissues, positions and their sizes, are inserted in the domain (2D model or 3D model) and the scattered field from the breast model is calculated as a forward problem using the FDFD method. The above scattered field is used to synthesize the measured scattered field values. Using the hybrid solution (FDFD/PSO) to find the position and the size of the maligant tissues as an inverse problem. The accuracy of the hybrid solution is excellent to get the same results as in forward problem. In all cases, the FDFD/PSO algorithm was able to find the proper position of the tumor.

5. CONCLUSION

In this paper, a proposed hybrid technique based on finite-difference frequency domain and particle swarm optimization technique is used for breast cancer detection. This technique is able to calculate the dimension and determine the position of the cancer in its early stage. Two-dimensional and three-dimensional models for the breast are used. The models include randomly distributed fatty breast tissue, glandular tissue, skin, as well as chest wall. They are characterized by the dielectric properties of the normal breast tissue and malignant tissue. Numerical results have been reported for two and three dimensional model. Results prove the possibility for attaining the localization and the size of the cancer inside the breast. The results are preliminary but promising.

REFERENCES

1. Gunnarsson, T., "Microwave imaging of biological tissues: Applied toward breast tumor detection," Malardalen Univeristy Licentiate Thesis, No. 73, Sweden, April 2007.
2. Fear, E. C., S. C. Hagness, P. M. Meaney, M. Okoiewski, and M. A. Stuchly, "Enhancing breast tumor detection with near-field imaging," *IEEE Microw. Magazine*, Vol. 3, No. 1, 48–56, Mar. 2002.
3. Liu, Q. H., Z. Q. Zhang, T. T. Wang, J. A. Brgan, G. A. Ybarra, L. W. Nolte, and W. T. Joines, "Active microwave imaging I — 2-D forward and inverse scattering methods," *IEEE Trans. Microwave Theory Tech.*, Vol. 50, No. 1, 123–133, Jan. 2002.
4. Qi, H. R. and N. A. Diakides, "Thermal infrared imaging in early breast cancer detection — A survey of recent research," *Proceeding of 25th Annual International Conference of IEEE*, Vol. 2, Issue 17–21, 1109–1112, Engeneering in Medicine and Biology Society, Sept. 2003.
5. Bindu, G., A. Lonappan, V. Thomas, C. K. Aanandan, and K. T. Matew, "Active microwave imaging for breast cancer detection," *Progress In Electromagnetics Research*, PIER 58, 419–169, 2006.
6. Yan, L., K. Huang, and C. Liu, "A noninvasive method for determining dielectric properties of layered tissues on human back," *J. of Electromagn. Waves and Appl.*, Vol. 21, No. 13, 1829–1843, 2007.
7. Wu, B.-I., F. C. Cox, and J. A. Kong, "Experimental methodology for non-thermal effects of electromagnetic radiation on biologics," *J. of Electromagn. Waves and Appl.*, Vol. 21, No. 13, 1829–1843, 2007.
8. Semenov, S. Y., et al., "Microwave tomography: Two-dimensional system for biological imaging," *IEEE Transactions on Biomedical Engineering*, Vol. 43, 869–877, 1996.
9. Hagness, S. C., A. Taflove, and J. E. Brdiges, "Two-dimensional FDTD analysis of a pulsed microwave confocal system for breast cancer detection: Fixed focus and antenna array sensors," *IEEE Transactions of Biomedical Engineering*, Vol. 45, 1470–1479, 1998.
10. Guo, B., Y. Wang, J. Li, P. Stoica, and R. Wu, "Microwave imaging via adaptive beamforming methods for breast cancer detection," *J. of Electromagn. Waves and Appl.*, Vol. 20, No. 1, 53–63, 2006.
11. Hagness, S. C., A. Taflove, and J. E. Brdiges, "Three-dimensional

FDTD analysis of a pulsed microwave confocal system for breast cancer detection: Design of an antenna array element," *IEEE Transactions of Antennas and Propagation*, Vol. 47, 783–791, 1999.

12. Fear, E. C., X. Li, S. C. Hagness, and M. A. Stuchly, "Confocal microwave imaging for breast cancer detection: Localization of tumors in three dimensions," *IEEE Transactions on Biomedical Engineering*, Vol. 49, 812–821, 2002.
13. Fear, E. C., J. Sill, and M. A. Stuchly, "Experimental feasibility of breast tumor detection and localization," *IEEE MTT-S Digest*, 383–386, 2003.
14. Fear, E. C., J. Sill, and M. A. Stuchly, "Experimental feasibility study of confocal microwave imaging for breast tumor detection," *IEEE Transactions on Microwave Theory and Techniques*, Vol. 51, 887–892, 2003.
15. Souvorov, A. E., A. E. Bulyshev, S. Y. Semenov, R. H. Svenson, A. G. Nazarov, Y. E. Sizov, and G. P. Tatsis, "Microwave tomography: A two-dimensional newton iterative scheme," *IEEE Trans. Microw. Theory Tech.*, Vol. 46, 1654–1659, 1998.
16. Chew, W. C. and Y. M. Wang, "Reconstruction of two-dimensional permittivity distribution using the distorted born iterative method," *IEEE Trans. Med. Imag.*, Vol. 9, 218–225, Jun. 1990.
17. Caorsi, S., A. Massa, M. Pastorino, and A. Rosani, "Microwave medical imaging: Potentialities and limitations of a stochastic optimization technique," *IEEE Trans. Microw. Theory Tech.*, Vol. 52, 1909–1916, 2004.
18. Xiao, F. and H. Yabe, "Microwave imaging of perfect conducting cylinders from real data by micro genetic algorithm coupled with deterministic method," *IEICE Trans. Electron.*, Vol. E81-C, 1784–1792, 1998.
19. Liu, X.-F., Y.-B. Chen, Y.-C. Jiao, and F.-S. Zhang, "Modified particle swarm optimization for patch antenna a design based on IE3D," *J. of Electromagn. Waves and Appl.*, Vol. 21, No. 13, 1819–1828, 2007.
20. Al-Sharkawy, M. H., V. Demir, and A. Z. Elsherbeni, "Plane wave scattering from three dimensional multiple objects using the iterative multiregion technique based on the FDFD method," *IEEE Trans. Antennas Propagat.*, Vol. 54, No. 2, 666–673, Feb. 2006.
21. Zainud-Deen, S. H., M. S. Ibrahim, and E. El-Deen, "A hybrid finite difference frequency domain and particle swarm

optimization techniques for forward and inverse electromagnetic scattering problems," *The 23rd Annual Review of Progress in Applied Computational Electromagnetics*, 1575–1580, Verona, Italy, March 19–23, 2007.

22. Zainud-Deen, S. H., E. El-Deen, and M. S. Ibrahem, "Electromagnetic scattering by conducting/dielectric objects," *The 23rd Annual Review of Progress in Applied Computational Electromagnetics*, 1866–1871, Verona, Italy, March 19–23, 2007.
23. Berenger, J.-P., "A perfectly matched layer for the absorption of electromagnetics waves," *J. Comput. Phys.*, Vol. 144, 185–200, Oct. 1994.
24. Robinson, J. and Y. Rahmat-Samii, "Particle swarm optimization in electromagnetics," *IEEE Trans. Antennas Propag.*, Vol. 52, 397–407, 2004.
25. Macea, J. R. and J. H. T. G. Fregnani, "Anatomy of thorocic wall, axillo and breast," *Int. J. Morphol.*, 691–704, Oct. 2006.
26. "Breast evaluation and treatment prevention early detection of breast cancer," University of Maryland Marlene and Stewart Greenebaum Cancer Center, 2005.
27. Zhang, Z. Q. and Q. H. Liu, "Microwave imaging for breast tumor: 2D forward and inverse methods," *IEEE Antennas Propag. Society International Symposium*, Vol. 1, 242–245, July 2001.
28. Xie, Y., B. Guo, L. Xu, J. Li, and P. Stocia, "Multistatic adaptive microwave imaging for early breast cancer detection," *IEEE Trans. Biomed. Eng.*, Vol. 53, No. 8, 1647–1657, Aug. 2006.
29. Hagness, S. C., A. Taflove, and J. E. bridges, "FDTD modeling of a coherent- addition antenna array for early-stage detection of breast cancer," *IEEE Antennas Propag. Society International Symposium*, Vol. 2, 1220–1223, June 1998.